

SIMUS: An open-source simulator for medical ultrasound imaging. Part II: Comparison with four simulators

Amanda Cigier, François Varray, Damien Garcia

▶ **To cite this version:**

Amanda Cigier, François Varray, Damien Garcia. SIMUS: An open-source simulator for medical ultrasound imaging. Part II: Comparison with four simulators. Computer Methods and Programs in Biomedicine, 2022, 220, pp.106726. 10.1016/j.cmpb.2022.106774 . hal-03702798

HAL Id: hal-03702798
https://cnrs.hal.science/hal-03702798

Submitted on 28 Jun 2022

HAL is a multi-disciplinary open access archive for the deposit and dissemination of scientific research documents, whether they are published or not. The documents may come from teaching and research institutions in France or abroad, or from public or private research centers.

L'archive ouverte pluridisciplinaire **HAL**, est destinée au dépôt et à la diffusion de documents scientifiques de niveau recherche, publiés ou non, émanant des établissements d'enseignement et de recherche français ou étrangers, des laboratoires publics ou privés.

SIMUS: An open-source simulator for medical ultrasound imaging. Part II: Comparison with four simulators

Amanda Cigier, François Varray, Damien Garcia

CREATIS: Centre de Recherche en Acquisition et Traitement de l'Image pour la Santé, Lyon, France

A B S T R A C T

Background and Objective: Computational ultrasound imaging has become a well-established methodology in the ultrasound community. In the accompanying paper (part I), we described a new ultrasound simulator (SIMUS) for MATLAB, which belongs to the Matlab UltraSound Toolbox (MUST). SIMUS can generate pressure fields and radiofrequency RF signals for simulations in medical ultrasound imaging. It works in a harmonic domain and uses far-field and paraxial linear equations.

Methods: In this article (part II), we illustrate how SIMUS compares with other ultrasound simulators (Field II, k-Wave, FOCUS, and Verasonics) for a homogeneous medium. We designed different transmit sequences (focused, planar, and diverging wavefronts) and calculated the corresponding 2-D and 3-D (with elevation focusing) RMS pressure fields.

Results: SIMUS produced pressure fields similar to those of Field II, FOCUS, and k-Wave. The acoustic fields provided by the Verasonics simulator were significantly different from those of SIMUS and k-Wave, although the overall appearance remained consistent.

Conclusion: Our simulations tend to demonstrate that SIMUS is reliable and can be used for realistic medical ultrasound simulations.

1. Introduction

Computational ultrasound imaging [1] has become popular since 2000 after the availability of the Field II [2] ultrasound simulator (Fig. 1 of Part I, [3]). The recent growing interest in computational ultrasound imaging is probably related to the accessibility of raw signals, driven by the emergence of ultrasound open platforms [4–7] dedicated to research (e.g. SARUS, UlaOP, Ultrasonix, Verasonics). The interplay between simulations and experimentations has fostered the development and validation of new techniques, both in transmit (e.g. coding, sparse arrays, transmission design) and in post-processing of ultrasound signals (e.g. beamforming, filtering, motion estimation). Access to realistic ultrasound simulations also enables teams not equipped with ultrasound scanners to participate and innovate in the processing of ultrasound signals. The potential offered by ultrasound simulations has motivated some investigators to address configurations not covered by Field II. Other simulators were then created, some of which have been mentioned in Part I. Among the open-source simulators, k-Wave quickly gained popularity and became another reference tool in computational ultrasound imaging. Based on the number of annual citations (Fig. 1 in Part I, [3]), k-Wave is now as widely adopted as Field II by the ultrasound imaging community. Although a substantial number of software packages have been developed to broaden the spectrum of simulated ultrasound conditions (a non-exhaustive list is given on the k-Wave website[1]), Field II and k-Wave are the most widely employed.

In the accompanying paper (part I), we introduced a new ultrasound simulator (SIMUS) that works in the harmonic domain and is written in MATLAB language [3]. SIMUS is part of the open-source MUST Matlab UltraSound Toolbox[2] that proposes codes for ultrasound experimentations and simulations [7]. The SIMUS program is based on far-field and paraxial equations and simulates radiofrequency RF signals for uniform linear or convex probes. SIMUS calls the function PFIELD that returns one-way (transmit) and two-way (transmit + receive) acoustic pressure fields. The theoretical aspect is described in detail in Part I. In particular, it is explained how the splitting of the transducer elements enables the use of far-field expressions. The RF signals can be analyzed with the open-source functions of the MUST toolbox [7] (beamforming [8], wall

☆ D.G. is also with INSERM (Institut National de la Santé Et de la Recherche Médicale). E-mails: damien.garcia@inserm.fr; garcia.damien@gmail.com.

E-mail addresses: francois.varray@creatis.insa-lyon.fr (F. Varray), damien.garcia@creatis.insa-lyon.fr (D. Garcia).

[1] http://www.k-wave.org/acousticsoftware.php

[2] https://www.biomecardio.com/MUST

Table 1
Properties of the Five Simulators.

	PFIELD	Field II	k-Wave	FOCUS	Verasonics
method	meshfree	meshfree	mesh	mesh	meshfree
acoustics	linear	linear	nonlinear	nonlinear	linear
time domain	harmonic	temporal	both	both	temporal
space domain	*x,y,z*	*x,y,z*	*x,y,z + k*	*x,y,z + k*	*x,y*
dimensionality	2D, 3D	3D	2D, 3D	3D	2D
scattering	weak	weak	multiple	–	weak
medium	homogeneous	homogeneous	heterogeneous	layered	homogeneous
open-source	yes	no	yes	no	no
free	yes	yes	yes	yes	no

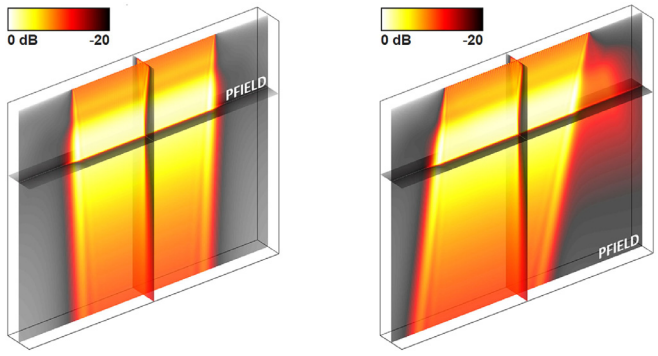


Fig. 1. Simulations of plane waves (tilt angles = 0°, 10°) transmitted by a 128-element linear array with PFIELD (see Table II). The maps represent the RMS (root mean square) acoustic pressure fields. They are 5-cm high.

filtering, Doppler [9], speckle tracking [10], etc.) to produce realistic ultrasound images. Some examples are provided in the accompanying paper and on the MUST website.

The objective of this part-II paper was to compare the one-way acoustic pressure fields returned by PFIELD with those simulated by Field II, k-Wave, and FOCUS [11]. We also included the Verasonics Research Ultrasound Simulator in the comparison protocol. Although the latter is a recent and therefore little cited [12] software, it could quickly gain popularity as the Verasonics research scanners are widely used by the ultrasound community. We consider it important that users be aware of how the Verasonics simulator differs from others. Since the theoretical background used in PFIELD/SIMUS is relatively close to that of Field II, except for the fact that SIMUS operates in the frequency domain, we also compared two-way PSFs (point-spread functions) generated by these two software packages. Before describing the comparison protocol and the results, we briefly review the theoretical and numerical specificities of the four simulators Field II, k-Wave, FOCUS, and Verasonics.

2. Field II, k-Wave, FOCUS, and Verasonics

Each ultrasound simulator has its own purpose and/or numerical specificity. Opting for one rather than the other depends essentially on the targeted goals, but also the ease of use and the realism of the simulations. The five ultrasound simulators that were compared (PFIELD, Field II, k-Wave, FOCUS, Verasonics) can all provide one-way acoustic pressure fields. In this study, we compared RMS (root mean square) acoustic pressures for standard emission sequences. We also compared two-way PSFs (SIMUS vs. Field II) after beamforming. We made two-way comparisons against Field II only, since Field II also uses a model based on point scatterers. The way PFIELD and SIMUS operate is explained in the part-I paper. Table 1 summarizes its features and those of the other three simulators.

2.1. Field II

J.A. Jensen introduced the MATLAB simulator Field in 1996 [2], which then became Field II, after a previous work on the simulation and validation of acoustic pressure fields generated by medical ultrasound transducers [13]. Field II works in the time domain and uses linear acoustics. The acoustic pressure field is calculated by dividing the transducer into small rectangular sub-elements and then summing their individual responses. For a given arbitrary point in the region of interest, Field II calculates the far-field spatial impulse response of a piston-like sub-element [14]. The acoustic pressure field at the same point is then deduced by convolving this local response with the excitation function of the transducer. The received responses are calculated from the acoustic reciprocity principle, by assuming that the point scatterers behave as monopole sources and do not interact with each other (weak scattering).

2.2. k-Wave

B.E. Treeby and B.T. Cox introduced the MATLAB toolbox k-Wave in 2010 [15], after a previous work on acoustic propagation models in heterogeneous media [16]. The toolbox k-Wave works in the k-space (wavenumber domain). The acoustic field is calculated at the nodes of regular mesh grids using both finite differences (over time) and a pseudo-spectral [17] method (in space). Point monopole sources and sensors are assigned to the grid points that belong to each transducer element. The received responses naturally derive from the numerical acoustic equations included in the software: backscattering occurs whenever an incident wave encounters an acoustic impedance gradient. In contrast to Field II and PFIELD, k-Wave can implicitly handle non-linear propagations and heterogeneous media [18]. Note, however, that some non-linear aspects were covered with add-ons to Field II [19,20] by considering only the fundamental and second harmonics and using the angular spectrum approach.

2.3. FOCUS

R.J. McGough introduced FOCUS to provide accurate pressure fields in the very near field where solving the acoustic equation can be a numerical issue. To this end, FOCUS uses the fast near-field method developed by the author [21]. The fast near-field method reduces a double integral – which is present in the impulse response approach – to a rapidly converging single integral and removes a singularity. The pressure fields are calculated on a grid by the angular spectrum approach. FOCUS can consider different transducer element geometries, layered media, and nonlinearity. Although one proceeding presented a comparison with Field II on a two-way example [22], the FOCUS software does not yet offer the possibility to simulate pulse-echo scenarios. The FOCUS software is not fully open as calculations are performed via compiled codes written in C++ and called by MATLAB functions.

Table 2
Simulated Conditions (one-way).

	0°-plane wave	10°-plane wave	diverging wave	focused wave
transducer	L11–5v (Verasonics)		P4–2v (Verasonics)	
center frequency	7.6 MHz		2.7 MHz	
elements	128		64	
kerf width	30 µm		50 µm	
element width	0.27 mm		0.25 mm	
pitch	0.3 mm		0.3 mm	
element height	5 mm (if 3-D)		1.4 cm (if 3D)	
elevation focus	1.8 cm (if 3-D)		6 cm (if 3D)	
two-way bandwidth	77%		74%	
TX focus	∞		(0,−1.64) cm	(3,5.2 cm)
TX apodization	boxcar		Tukey	boxcar

2.4. Verasonics

The Verasonics Vantage ultrasound scanners are probably the most widely used research scanners for ultrasound medical imaging. Their flexibility and accessibility to raw ultrasound data make them well suited for 2-D and 3-D ultrasound research. Verasonics recently introduced its ultrasound simulator software. It is likely to become increasingly popular as it is integrated into the Vantage platform, which is why we have chosen to include this simulator in our comparison panel. To date, there is no theoretical document that describes the Verasonics simulator. According to the Verasonics website [23], the Verasonics simulator simulates backscattered echoes from a set of point targets with a given reflectivity. The contributions of each emitting element are summed by assuming linear acoustic propagation. In the Verasonics simulator, the transmit waveform, the transmit and receive apodizations, as well as the directivities of the elements are considered to simulate RF signals. The website does not specify whether the simulator applies 2-D or 3-D equations. Since the values of the element height and elevation focus did not modify the acoustic pressures, we postulated that the Verasonics simulator is 2-D.

3. Method: comparison of the four simulators

3.1. One-way configurations: acoustic pressure fields

We compared the five ultrasound simulators PFIELD, Field II, k-Wave, FOCUS, and Verasonics, by simulating acoustic pressure fields with four different short-pulse emission patterns: plane waves with a tilt angle of 0° or 10°, diverging wave, and focused wave. The properties of the transducers and transmits are summarized in Table 2. We tested either 2-D or 3-D conditions or both, depending on the simulator characteristics. Two ultrasound transducers were simulated, a linear and a phased array. Their properties (Table II) were those of the L11–5v and P4–2v Verasonics transducers. The medium was homogeneous and non-attenuating, with a speed of sound of 1540 m/s. Note that the current versions of PFIELD and SIMUS cannot handle inhomogeneous media but can consider attenuation. The excitation pulse length was of one wavelength (see Fig. 8 in part I, [3]). To ensure similar transmit conditions between the software packages, the pulse generated by PFIELD was used as pressure input to the other simulators. We simulated RMS (root mean square) acoustic pressure fields and compared them on a decibel dB scale. All pressure fields were normalized so that their maxima were equal to one. The pressure points were located on Cartesian grids with steps of approximately half a wavelength in the x- and z-directions, and one sixth of a wavelength in the y-direction. The transducer elements were split in both x- and y-directions for Field II and k-Wave (to obtain 2×17 sub-elements). The elements were not split in the x-direction in FOCUS since a near-field method is used [11]. It is recalled that dividing the elements in the y-direction enables a focus in elevation (see Part I for more details). On the other hand, the elements were not split in the y-direction with PFIELD since it applies continuous delays along the elevation direction (see Equation (4) in part I). To compare PFIELD with the other simulators, we calculated the absolute pressure differences in the dB scale as $20 \log(|P(\text{PFIELD}) - P(\text{other})|)$, after normalization. To obtain a global comparison, we pooled all simulated pressure field values from the same simulator (for 2-D and 3-D, respectively), and calculated the inter-simulator correlation coefficients. To reduce biased trends induced by the lowest values, only acoustic pressures above -20 dB were taken into account in the calculation of the correlation coefficients.

3.2. Two-way configurations: PSF

SIMUS simulates radio-frequency RF signals from the function PFIELD. We also compared SIMUS and Field II in two-way configurations by calculating two-way PSFs (point-spread functions). A two-way PSF was defined as the real envelope returned by a single scatterer after beamforming. We tested two ultrasound 3-D conditions: an unsteered plane wave with a L11–5v linear array (Table II, leftmost column) and a focused wave with a P4–2v phased array focusing at 6 cm deep (Table II, rightmost column). To investigate the two-way PSFs, one scatterer was located at (0 cm; 2 cm) and (0 cm; 6 cm) in the plane- and focused-wave configurations, respectively. The simulated RF signals were I/Q demodulated and beamformed with a delay-and-sum (DAS) [8]. During beamforming, we used a receive f-number of 1.5 with the linear array, while a full aperture was used with the phased array. We calculated the absolute differences of the PSF in the dB scale as $20 \log(|\text{PSF(SIMUS)} - \text{PSF(Field II)}|)$.

4. Results

Fig. 1 to Fig. 7 show the simulated acoustic pressure maps and the absolute differences with respect to PFIELD. We observed a good concordance between PFIELD, Field II, k-Wave, and FOCUS with the 3-D simulations ($r^2 \geq 0.93$). There was also a good concordance between PFIELD and k-Wave under 2-D conditions. The 2-D acoustic pressure fields simulated by the Verasonics ultrasound simulator were significantly different from those generated by PFIELD and k-Wave. In 3-D, when considering all simulations, the squares of the inter-simulator correlation coefficients were all greater than 0.97 (PFIELD vs. Field II vs. k-Wave, Fig. 8). The correlation between PFIELD and k-Wave was lesser in 2-D ($r^2 = 0.89$), as side lobes were more visible with PFIELD than with k-Wave (Fig. 4, bottom). The 2-D correlation coefficients associated with the Verasonics simulator were the smallest ($r^2 < 0.77$). The two-way PSFs returned by SIMUS and Field II are displayed in Fig. 9 and Fig. 10.

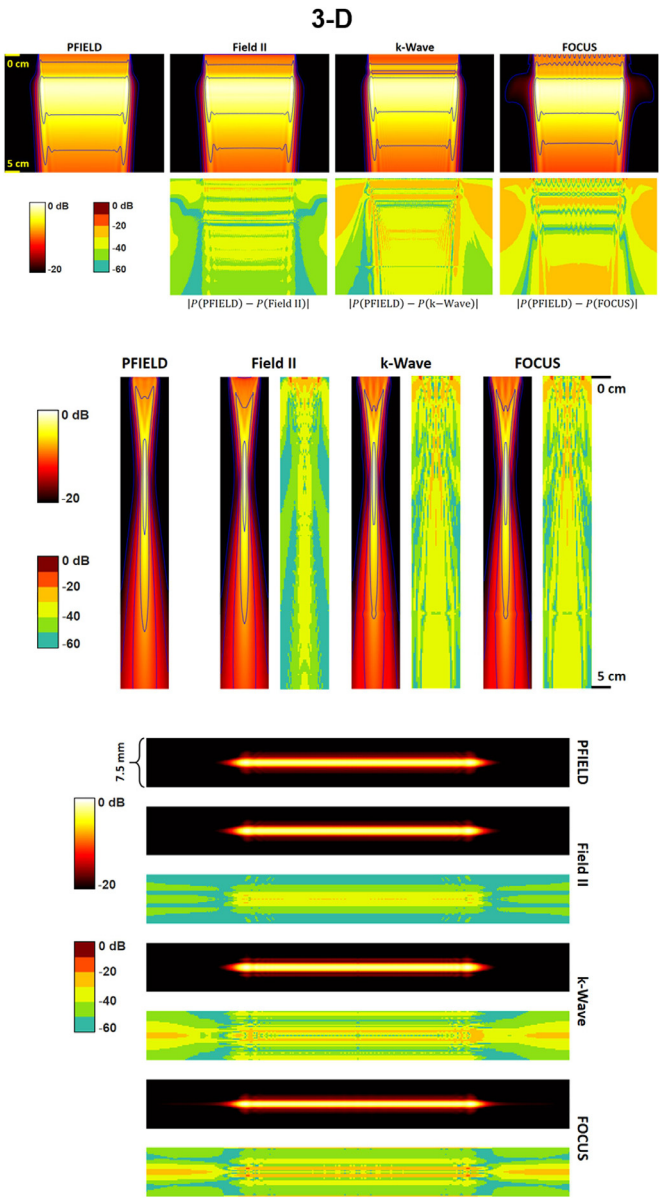


Fig. 2. 3-D simulations: comparison between PFIELD, Field II, k-Wave, and FOCUS for the 0°-tilt plane wave (see Fig. 1, left). The three planes are those displayed in Fig. 1, left. From top to bottom: azimuthal plane, elevation plane, focal plane. The green-to-red maps represent the absolute differences with respect to PFIELD.

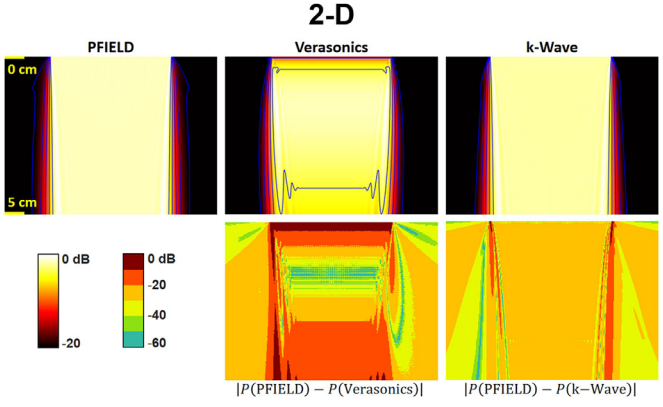


Fig. 3. 2-D simulations: comparison between PFIELD, Verasonics, and k-Wave for the 0°-tilt plane wave. The second row represents the absolute differences with respect to PFIELD.

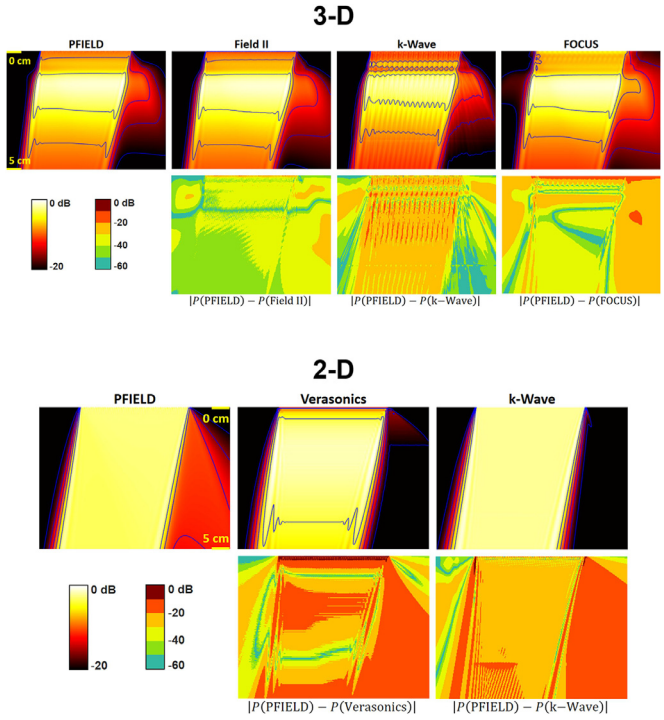


Fig. 4. 3-D (top) and 2-D (bottom) simulations of a 10°-tilt plane wave. A 3-D overview is given in Fig. 1, right. The second rows represent the absolute differences with respect to PFIELD.

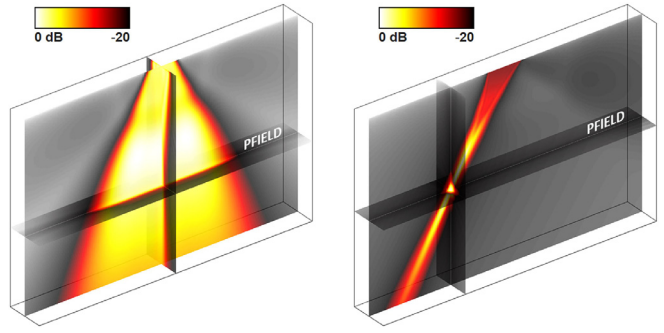


Fig. 5. Simulations of diverging and focused waves transmitted by a 64-element phased array with PFIELD (see also Table II). The maps represent the RMS (root mean square) acoustic pressure fields. They are 10-cm high.

They were very similar in both plane-wave and focused-wave configurations.

The computing times were significantly different from one simulator to another. It should be noted that the notion of calculation time is somewhat subjective. Each software has its specific applications, and proposes its own numerical tricks to reduce the computation time, generally at the expense of the accuracy. In this paper, we have focused on accuracy. In addition, each software can be run in parallel, with different algorithmic strategies. An exhaustive comparative study would require testing several test cases, each with several tuning parameters and operating systems. As an indication only (and under the request of reviewers), the computing times on the same personal laptop (non-parallel computations) were for the "plane wave" sequence (Fig. 1): PFIELD: 260 s, Field II: 480 s, k-Wave: 11600 s (380 s in parallel), FOCUS: 1700 s; for the "diverging wave" sequence (Fig. 6): PFIELD: 15 s, Field II: 80 s, k-Wave: 73,600 s (1700s in parallel), FOCUS: 2100 s.

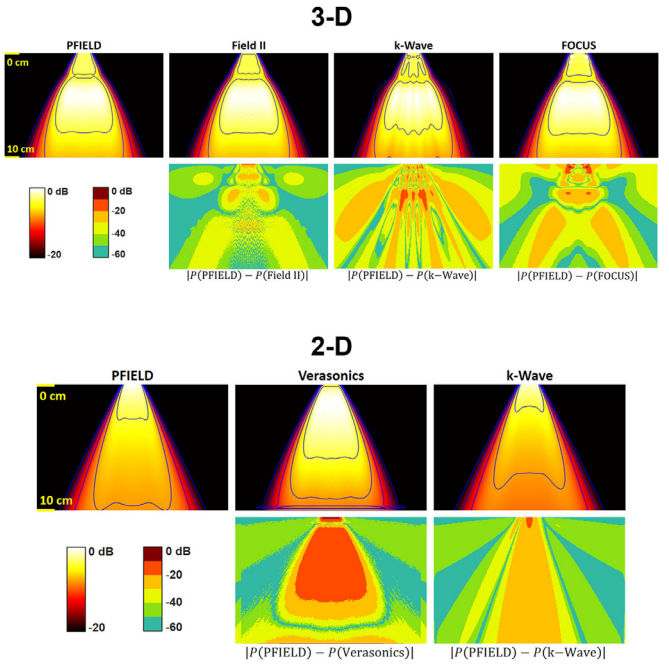


Fig. 6. 3-D (top) and 2-D (bottom) simulations of a diverging wave. A 3-D overview is given in Fig. 5, left. The second rows represent the absolute differences with respect to PFIELD.

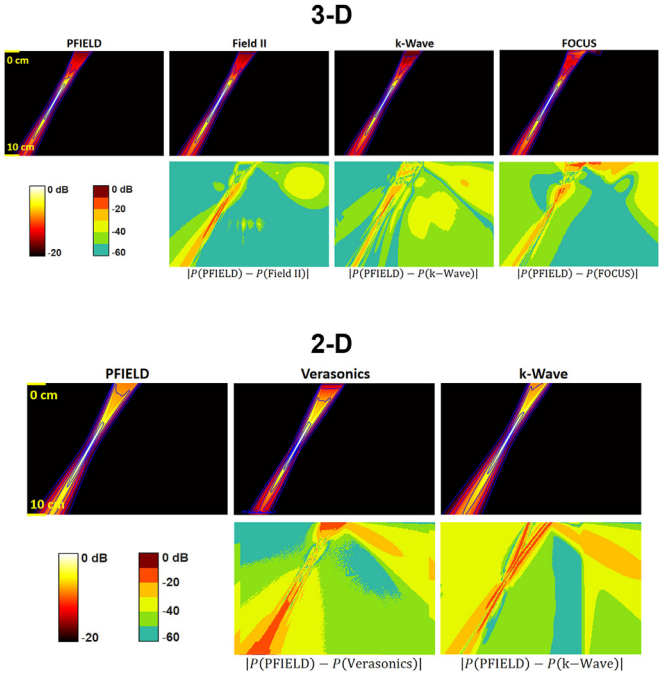


Fig. 7. 3-D (top) and 2-D (bottom) simulations of a focused wave. A 3-D overview is given in Fig. 5, right. The second rows represent the absolute differences with respect to PFIELD.

5. Discussion

The new ultrasound simulator SIMUS generated acoustic pressure fields similar to those simulated by the other software packages Field II, k-Wave, and FOCUS, especially in 3-D ($r^2 > 0.92$, Fig. 8). Like these popular ultrasound simulators, SIMUS can therefore be considered to produce synthetic medical ultrasound signals, under the conditions described in parts I and II (linearity, homogeneous medium, etc.).



Fig. 8. Overall comparison between the five simulators after pooling all simulated acoustic pressures. The numbers are the squared correlation coefficients (r^2).

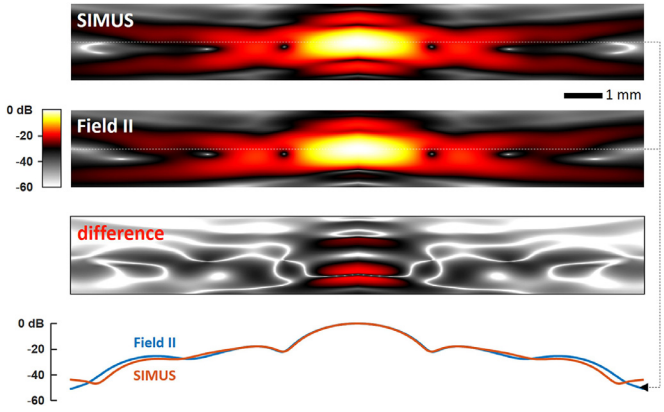


Fig. 9. Comparison of two-way PSFs (SIMUS vs. Field II) in a focused-wave configuration with a simulated phased array.

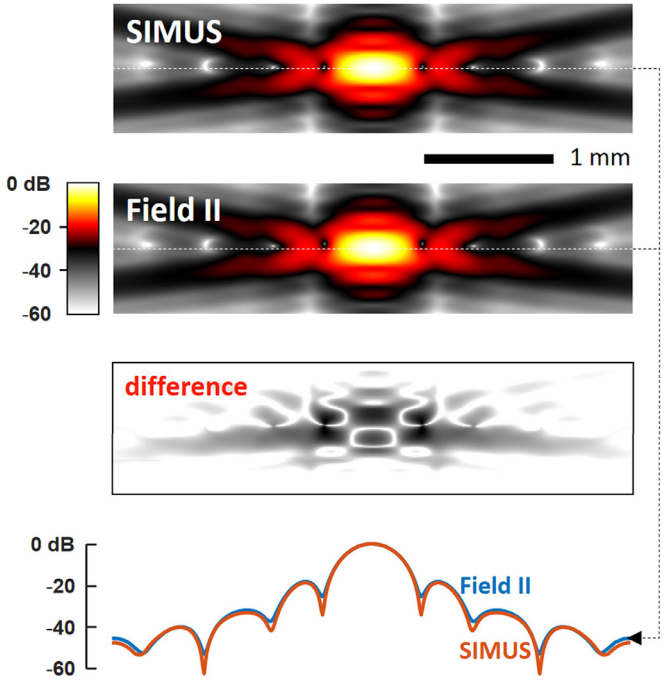


Fig. 10. Comparison of two-way PSFs (SIMUS vs. Field II) in a plane-wave configuration with a simulated linear array.

Under 2-D conditions, although the radiation patterns appeared to be identical, we observed some differences with the Verasonics simulator ($r^2 < 0.77$, Fig. 8). Regarding the differences found with the Verasonics commercial simulator, it is difficult to give a justification because, unlike Field II, k-Wave, and FOCUS, the theoretical and numerical methods are not publicly available. The best match

was with Field II. This is unsurprising because we founded SIMUS based on the same assumptions as Field II, namely: linearity, homogeneity, and far-field equations with the use of sub-elements. Like Field II, SIMUS uses weak and monopole scattering. It follows that the two-way PSFs obtained with SIMUS and Field II were similar. The main numerical difference between PFIELD/SIMUS and Field II is the computational domain: temporal with Field II, frequency with SIMUS. The frequency domain is indeed appropriate when dealing simulations with signals with bandpass signals. It can also easily consider acoustical features that depend on the frequency, such as the directivity of the elements, attenuation in the tissues, or Rayleigh scattering, for example. Another difference appears with regard to elevation focusing. In SIMUS, to simulate focusing in the elevation direction, we adjusted the velocity delays of the pistons along their height (see Fig. 4 in the accompanying part-I paper), as suggested in [24]. In Field II, the elements are split into sub-elements in the height direction. A transmission delay is associated with each of these sub-elements to provide focusing in elevation. A similar strategy is used in k-Wave.

It is important to note that the correlation coefficients reported in Fig. 8 characterize the inter-simulator similarities that we observed with a large and deep medium. The dimensions of the medium we chose are those typically encountered in B-mode or Doppler imaging. A smaller coefficient between two simulators means that they give substantially different results under these particular conditions. It does not imply that one of them is "inferior". It was difficult to compare the simulators under optimal conditions given that they each have distinct numerical characteristics. To achieve comparisons that were as fair as possible, we chose sufficiently fine grids. This strategy did not allow us to take into account the very near field, for which FOCUS and k-Wave are expected to be better adapted than Field II and PFIELD. A much finer grid (and much longer computation time) would have been necessary to examine the nearby region. In most medical imaging cases, however, it is not needed to achieve high-accuracy simulations at the near-field because the thicknesses of the acoustic matching layer and lens ($\sim$1 mm for a linear transducer) [25], and that of the skin ($\sim$0.5 mm), separate the scanned region by several wavelengths from the surface of the transducers. As shown in the appendix of part I (Figures 14 and 15), the radiation fields from PFIELD approximate well those calculated by the Rayleigh-Sommerfeld integral beyond a distance of two wavelengths (relative errors $<$ 3%). These results confirm that the far-field equation can be used when slicing the transducer elements [24].

5.1. When using simus and PFIELD?

SIMUS and PFIELD are part of the MATLAB Ultrasound Toolbox MUST toolbox [7]. This toolbox, as illustrated by the numerous examples available on the website,[3] allows students and researchers to quickly learn experimental ultrasound imaging: acquisitions, demodulation, beamforming, wall filtering, color Doppler, vector Doppler, speckle tracking… SIMUS and PFIELD complete the series by offering to perform realistic ultrasound simulations for pedagogical and research purposes. In contrast to Field II, the MATLAB codes are open and highly documented. The default functions allow many tasks to be performed, such as those illustrated by the examples in the Part-I paper. An advanced user can modify the codes or the programming language according to her needs. PFIELD and SIMUS have been already used in several published works. For example, far-field patterns were generated with PFIELD to design diverging-wave transmit sequences for high-frame-rate motion-compensated echocardiography in human hearts [26]. Vector flow imaging with vector Doppler was simulated in a carotid bifurcation by coupling SIMUS with an SPH (smoothed particle hydrodynamics) flow model [27]. In our team, SIMUS has also recently been applied in the generation of simulated moving ultrasound phantoms and left ventricles to train convolutional neural networks for motion estimation in echocardiography [28,29]. We also simulated clinical-type Doppler-echo cineloops with the future objective to train deep learning algorithms for intracardiac flow imaging [30]. In the same vein, Milecki *et al.* trained a convolutional neural network by using SIMUS simulations in a synthetic murine brain microvascular network for deep-learning-based ultrasound localization microscopy [31].

[3] https://www.biomecardio.com/MUST

5.2. What simus cannot do, what it can

Like Field II and k-Wave, SIMUS can be used to produce realistic radiofrequency RF signals for pulse-echo ultrasound imaging. Only linear acoustics into homogeneous media, however, is considered in the current version of SIMUS. The homogeneity hypothesis means that both density and speed of sound are constant. Aberrations due to acoustic impedance gradients thus cannot be simulated at the time of publication of this article. The linearity assumption simplifies the problem since it allows the summation of the time-harmonic solutions, but this prevents one from addressing non-linear properties as in harmonic imaging. SIMUS also considers only weak (single) scattering to avoid computational overload of multiple scattering. The multiple reverberation artifacts, which are sometimes observed in clinical ultrasound, therefore cannot be simulated. In contrast, the simulator k-Wave can account for nonlinearity, acoustic heterogeneities, and multiple scattering. However, because k-Wave uses a mesh-based method, the locations of the scatterers are linked to the geometry of the grid. This represents a major difference with SIMUS (or Field II), which is a particle-based software. In SIMUS, the speckles of the B-mode images result from the pseudorandom positions of the scatterers, while they are due to local changes in impedance in k-Wave. In addition to numerical simplifications, the use of a particle-based model readily allows the motion of individual particles. This makes it an ideal simulation method for tissue displacements and the investigation of ultrasound techniques for motion analysis (e.g. speckle tracking [28], Doppler [32], vector flow imaging [27]).

Although SIMUS is able to consider near fields through element splitting (see accompanying paper, part I, [3]), the singularity related to the 1/r term present in the equations does not allow for evaluations near the surface of the transducer. A free software such as FOCUS removes this singularity and offers high accuracy in the very near field regions [21]. As explained in a previous paragraph, this aspect is not a limitation for ultrasound medical imaging for which this specific region is generally not investigated.

5.3. Potential future perspectives

In creating SIMUS, our intention was not to be "better" or more innovative than other simulators. As we mentioned earlier, each ultrasound simulator has its own specificity. Our first goal was to release an open-source MATLAB toolbox (MUST) for students and researchers in ultrasound imaging [7]. To make it self-contained, we intended this toolbox to include a reliable, open-code ultrasound simulator that is sufficiently documented to make users aware of its capabilities and limitations. From the comparative results described in the present work, it appears that SIMUS can be used for medical ultrasound research. Since the MUST toolbox is available online, PFIELD and SIMUS have been used or tested by researchers and students on several continents (Fig. 11). The present SIMUS version is for 1-D uniform (convex or linear) arrays. Depending on

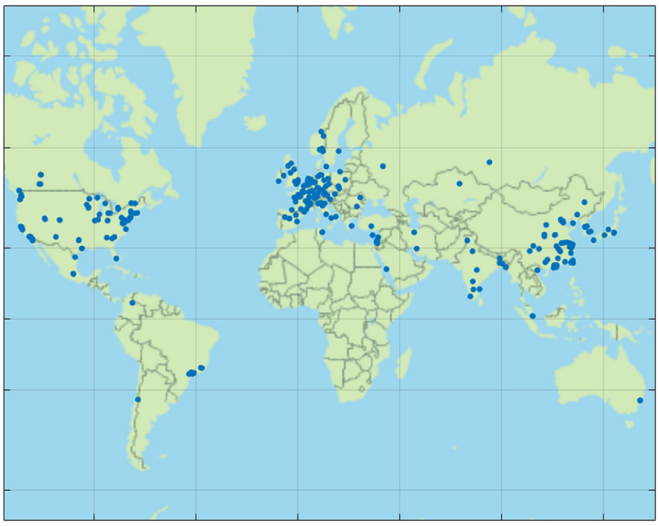


Fig. 11. Cities where SIMUS has been used (2022/03).

the success of SIMUS, we will incorporate the option to simulate matrix arrays for volume ultrasound imaging. A partition of the elements in the *Y*-direction of elevation will then be necessary to enable the use of the far field equations (see accompanying paper, part I). Similarly, a future version will allow the positioning and orientation of the elements at the user's convenience. Such an update would allow completing the medical imaging spectrum by considering, for example, sparse arrays or ultrasound computer tomography. It is understood that these updates will significantly increase the number of element-scatterer interactions. Some numerical strategies will have to be implemented to reduce the computation time. As we are interested in the simulation of cardiac images (echocardiography), we may also plan to integrate an add-on for the calculation of the second harmonic using a quasi-linear approximation of the nonlinear wave propagation [33,34]. Finally, by using a geometric ray-tracing method based on the eikonal approximation, generating non-homogeneous media would also be conceivable. This approach could be applied to derive artifacts due to aberrations, or to investigate quantitative ultrasonography methods such as the local measurement of the propagation speed.

As artificial intelligence has gained momentum in medical imaging, ultrasound simulations have found a new interest through deep learning. In medical imaging, whether ultrasound or other, the main challenge is to train neural networks with hundreds or thousands of images, which are sometimes difficult to access. Rather than being based on patient data, training can be done through patient-like simulations whose number is limited by computational time only. The key task is then to obtain simulations that are realistic enough to fool the network. "Realistic" does not mean "exact". A simulator is sufficiently "realistic" if images or signals similar to those obtained in a patient (e.g., RF or I/Q signals, B-mode or color Doppler images) can be simulated. It is understood that the subjective degree of realism depends on the intended goal. The network will then be functional when dealing with real clinical images. If simulated signals or images can be used to train neural networks with limited effort, we anticipate that ultrasound simulators still have a bright future ahead of them.

6. Conclusion

The open-source MATLAB simulator SIMUS is efficient and easy to use. Like Field II, k-Wave, and FOCUS, SIMUS could contribute to the growing popularization of computational ultrasound imaging.

Acknowledgment

This work was supported in part by the LABEX CeLyA (ANR-10-LABX-0060) of Université de Lyon, within the program "Investissements d'Avenir" (ANR-16-IDEX-0005) operated by the French National Research Agency.

References

[1] M. Verweij, B. Treeby, L. Demi, Simulation of ultrasound fields, in: Comprehensive Biomedical Physics, 2, Elsevier, Oxford, 2014, pp. 465–499, doi:10.1016/B978-0-444-53632-7.00221-5.

[2] J.A. Jensen, FIELD: a program for simulating ultrasound systems, in: 10th Nordicbaltic Conference on Biomedical Imaging, 1996, pp. 351–353. Vol. 4, Supplement 1, Part 1:351–353.

[3] D. Garcia, SIMUS: an open-source simulator for medical ultrasound imaging. Part I: theory & examples, Comput Methods Programs Biomed (2022) 106726, doi:10.1016/j.cmpb.2022.106726.

[4] P. Tortoli, L. Bassi, E. Boni, A. Dallai, F. Guidi, S. Ricci, ULA-OP: an advanced open platform for ultrasound research, IEEE Trans Ultrason Ferroelectr Freq Control 56 (10) (2009) 2207–2216, doi:10.1109/TUFFC.2009.1303.

[5] J.A. Jensen, et al., SARUS: a synthetic aperture real-time ultrasound system, IEEE Trans Ultrason Ferroelectr Freq Control 60 (9) (2013) 1838–1852, doi:10.1109/TUFFC.2013.2770.

[6] E. Boni, A.C.H. Yu, S. Freear, J.A. Jensen, P. Tortoli, Ultrasound open platforms for next-generation imaging technique development, IEEE Trans Ultrason Ferroelectr Freq Control 65 (7) (2018) 1078–1092, doi:10.1109/TUFFC.2018.2844560.

[7] D. Garcia, Make the most of MUST, an open-source Matlab UltraSound Toolbox, in: 2021 IEEE International Ultrasonics Symposium (IUS), 2021, pp. 1–4, doi:10.1109/IUS52206.2021.9593605.

[8] V. Perrot, M. Polichetti, F. Varray, D. Garcia, So you think you can DAS? A viewpoint on delay-and-sum beamforming, Ultrasonics 111 (2021) 106309, doi:10.1016/j.ultras.2020.106309.

[9] C. Madiena, J. Faurie, J. Porée, D. Garcia, Color and vector flow imaging in parallel ultrasound with sub-Nyquist sampling, IEEE Trans Ultrason Ferroelectr Freq Control 65 (5) (2018) 795–802, doi:10.1109/TUFFC.2018.2817885.

[10] V. Perrot, D. Garcia, Back to basics in ultrasound velocimetry: tracking speckles by using a standard PIV algorithm, in: 2018 IEEE International Ultrasonics Symposium (IUS), 2018, pp. 206–212, doi:10.1109/ULTSYM.2018.8579665.

[11] R.J. McGough, Rapid calculations of time-harmonic nearfield pressures produced by rectangular pistons, J. Acoust. Soc. Am. 115 (5) (2004) 1934–1941, doi:10.1121/1.1694991.

[12] C. Huang, et al., Simultaneous noise suppression and incoherent artifact reduction in ultrafast ultrasound vascular imaging, IEEE Trans Ultrason Ferroelectr Freq Control (2021), doi:10.1109/TUFFC.2021.3055498.

[13] J.A. Jensen, N.B. Svendsen, Calculation of pressure fields from arbitrarily shaped, apodized, and excited ultrasound transducers, IEEE Trans Ultrason Ferroelectr Freq Control 39 (2) (1992) 262–267, doi:10.1109/58.139123.

[14] P.R. Stepanishen, Transient radiation from pistons in an infinite planar baffle, J. Acoust. Soc. Am. 49 (5B) (1971) 1629–1638, doi:10.1121/1.1912541.

[15] B.E. Treeby, B.T. Cox, k-Wave: MATLAB toolbox for the simulation and reconstruction of photoacoustic wave fields, JBO, JBOPFO 15 (2) (2010) 021314, doi:10.1117/1.3360308.

[16] B.T. Cox, S. Kara, S.R. Arridge, P.C. Beard, k-space propagation models for acoustically heterogeneous media: application to biomedical photoacoustics, J. Acoust. Soc. Am. 121 (6) (2007) 3453–3464 Jun, doi:10.1121/1.2717409.

[17] L.N. Trefethen, Spectral methods in MATLAB, Society for Industrial and Applied Mathematics (2000), doi:10.1137/1.9780898719598.

[18] B.E. Treeby, J. Jaros, A.P. Rendell, B.T. Cox, Modeling nonlinear ultrasound propagation in heterogeneous media with power law absorption using a k-space pseudospectral method, J. Acoust. Soc. Am. 131 (6) (2012) 4324–4336, doi:10.1121/1.4712021.

[19] Y. Du, J.A. Jensen, Feasibility of non-linear simulation for Field II using an angular spectrum approach, in: 2008 IEEE Ultrasonics Symposium, 2008, pp. 1314–1317, doi:10.1109/ULTSYM.2008.0318.

[20] Y. Du, R. Fan, Y. Li, S. Chen, J.A. Jensen, A framework for simulating ultrasound imaging based on first order nonlinear pressure-velocity relations, Ultrasonics 69 (2016) 152–165, doi:10.1016/j.ultras.2016.03.015.

[21] D. Chen, R.J. McGough, A 2D fast near-field method for calculating near-field pressures generated by apodized rectangular pistons, J Acoust Soc Am 124 (3) (2008) 1526–1537, doi:10.1121/1.2950081.

[22] Y. Zhu, T.L. Szabo, R.J. McGough, A comparison of ultrasound image simulations with FOCUS and Field II, in: 2012 IEEE International Ultrasonics Symposium, 2012, pp. 1694–1697, doi:10.1109/ULTSYM.2012.0425.

[23] M. Vega, Ultrasound simulator software, Verasonics (2022) https://verasonics.com/ultrasound-simulator/.

[24] L.W. Schmerr Jr, Fundamentals of Ultrasonic Phased Arrays, Springer International Publishing, 2015.

[25] R.E. McKeighen, in: Design Guidelines For Medical Ultrasonic Arrays, San Diego, CA, 1998, pp. 2–18, doi:10.1117/12.307992.
[26] J. Porée, D. Posada, A. Hodzic, F. Tournoux, G. Cloutier, D. Garcia, High-frame-rate echocardiography using coherent compounding with Doppler-based motion-compensation, IEEE Trans Med Imaging 35 (7) (2016) 1647–1657, doi:10.1109/TMI.2016.2523346.
[27] S. Shahriari, D. Garcia, Meshfree simulations of ultrasound vector flow imaging using smoothed particle hydrodynamics, Phys Med Biol 63 (2018) 1–12, doi:10.1088/1361-6560/aae3c3.
[28] E. Evain, K. Faraz, T. Grenier, D. Garcia, M.D. Craene, O. Bernard, A pilot study on convolutional neural networks for motion estimation from ultrasound images, IEEE Trans Ultrason Ferroelectr Freq Control 67 (12) (Dec. 2020) 2565–2573, doi:10.1109/TUFFC.2020.2976809.
[29] E. Evain, et al., Motion estimation by deep learning in 2D echocardiography: synthetic dataset and validation, IEEE Trans Med Imaging (2022) 1–14, doi:10.1109/TMI.2022.3151606.
[30] Y. Sun, et al., A pipeline for the generation of synthetic cardiac color Doppler, IEEE Trans Ultrason Ferroelectr Freq Control (2022) 1–10, doi:10.1109/TUFFC.2021.3136620.
[31] L. Milecki, et al., A deep learning framework for spatiotemporal ultrasound localization microscopy, IEEE Trans Med Imaging 40 (5) (2021) 1428–1437, doi:10.1109/TMI.2021.3056951.
[32] F. Mehregan, et al., Doppler vortography: a color Doppler approach to quantification of intraventricular blood flow vortices, Ultrasound Med Biol 40 (1) (2014) 210–221, doi:10.1016/j.ultrasmedbio.2013.09.013.
[33] H. Torp, T. Johansen, J.S. Haugen, Nonlinear wave propagation - a fast 3D simulation method based on quasi-linear approximation of the second harmonic field, in: 2002 IEEE Ultrasonics Symposium, 2002. Proceedings., 1, 2002, pp. 567–570, doi:10.1109/ULTSYM.2002.1193467.
[34] F. Varray, A. Ramalli, C. Cachard, P. Tortoli, O. Basset, Fundamental and second-harmonic ultrasound field computation of inhomogeneous nonlinear medium with a generalized angular spectrum method, IEEE Trans Ultrason Ferroelectr Freq Control 58 (7) (2011) 1366–1376, doi:10.1109/TUFFC.2011.1956.